

## Promoting Fertilizer Use via Controlled Release of a Bacteria-Encapsulated Film Bag

CHIN-SAN WU\*

Department of Chemical and Biochemical Engineering, Kao Yuan University, Kaohsiung County, Taiwan 82101, Republic of China

A phosphate-solubilizing bacterium (*Burkholderia cepacia* isolate) encapsulated in maleic anhydride (MA) grafted onto poly(butylene succinate adipate) (PBSA) and then combined with starch as film bag material (PBSA-*g*-MA/starch) incubated in a saline solution required approximately 20 days to deplete the starch in the film bags. Thereafter, the cell concentration in the saline solution increased significantly because of the release of cells from the severely destroyed film bags and also their growth by use of depolymerized PBSA-*g*-MA fragments as a substrate. The incubation proceeded for 60 days, by which time the PBSA-*g*-MA/starch composite had suffered a >80% weight loss. For practical application, effectiveness of the above-mentioned film bags was demonstrated because it could improve the absorbability of a fertilizer for plants and promote the growth of plants. As a result, it can avoid the accumulation of the phosphate in excess fertilizer that lead to the phenomenon of poor soils. These results demonstrate that PBSA-*g*-MA/starch can be used to encapsulate cells of an indigenous phosphate-solubilizing bacterium (*B. cepacia* isolate) to form a controlled release of bacteria-encapsulated film bag (BEFB). The *B. cepacia* isolate was able to degrade the film bags material, causing cell release. Biodegradability of the film bags depended upon the type of material used, because the PBSA film bags were also degraded but to a lesser degree. The addition of starch made the film bags more biodegradable. The decrease in intrinsic viscosity was also higher for the starch composite, suggesting a strong connection between the biodegradability and these characteristics. The results suggest that the release of fertilizer-promoted bacteria might be controllable via a suitable film bag material formulation. In addition, this work adopted live bacteria to promote the absorption of phosphate, which is superior to the phosphate used in the traditional way.

**KEYWORDS:** Poly(butylene succinate adipate) (PBSA); phosphate-solubilizing bacterium (PSB); biodegradation; controlled release; bacteria-encapsulated film bag (BEFB)

### INTRODUCTION

One of the essential macronutrients required for the growth of plants is phosphorus, whose deficiency will restrict plant growth in soil (1), but the excessive addition of chemically synthesized fertilizers for crop production has led to the deterioration of farmland quality because of insoluble phosphate complexes in the soil. This problem has motivated the use of more environmentally friendly fertilizers for sustainable land use, of which phosphate-solubilizing bacteria (PSBs) are one of the most popular choices for bacteria-encapsulated film bag (BEFB) (2, 3). PSBs were bacteria-promoted fertilizers that help to break down the phosphate particles to become smaller and then make it easier to assimilate by the plant roots (4–6). PSBs can solubilize and mobilize insoluble phosphate compounds accumulated in soil through biotic acidification, chelation, and exchange reactions (7, 8), thereby allowing crops to use the soluble phosphate compounds released from the soil without the need for additional phosphate fertilizers.

However, developing an effective method to inoculate bacteria into the soil and maintaining viability and function of these bacteria in the soil during crop cultivation are still needed. The best of both worlds can be achieved by encapsulating the bacterial cells in biodegradable film bags, which protect the cells while allowing their release into the soil in a controlled manner. As a result, the effectiveness and stability of BEFB can be enhanced markedly. A key issue in the development of “controlled-release” BEFB, however, is developing and designing suitable biodegradable materials for controlled-release film bags.

Among the commercialized biodegradable plastics, poly(butylene succinate adipate) (PBSA) has received a great deal of attention because of its mechanical properties and biodegradability, as well as its hydrophobic nature (9, 10), but its high production cost appears to limit its commercial applications. This limitation can be overcome by blending PBSA with cost-effective biodegradable natural biopolymers, such as starch, cellulose, and wood fiber, to create new materials with the desired properties (11–15). In particular, starch is used most often because it is abundant, inexpensive, renewable, and fully biodegradable. Blending PBSA and starch could markedly reduce

\*To whom correspondence should be addressed. Telephone: +886-7-6077685. Fax: +886-7-6077788. E-mail: cws1222@cc.kyu.edu.tw.

the cost and enable flexibility in adjusting the biodegradability and mechanical properties of the hybrid products, but because starch is fairly hydrophilic, the poor compatibility between the two phases could cause problems. Therefore, the addition of a compatibilizer or a toughener is usually needed to enhance the compatibility of the two immiscible phases, resulting in better mechanical properties of the composite (16). The literature shows that maleic anhydride (MA)-grafted polylactide (17) could be used for this purpose. PBSA, which is condensed by adipic acid glycol and succinic acid with 1,4-butanediol through esterification and deglycolization, is a candidate biodegradable polyester and could replace non-biodegradable and general polymers, such as polystyrene and polyethylene (18).

In this study, PBSA as the core matrix was blended with starch to modify its physical properties, including biodegradability and permeability. To decide on a compatibilizer and/or a toughener to overcome the poor adhesion starch–polymer composites, the MA-grafted composite, PBSA-g-MA/starch, was compared to PBSA. Both were used to encapsulate cells of an indigenous PSB strain (*Burkholderia cepacia*), and changes in the structure and biodegradability of the film bags in saline solution and in fertilizer solution or cultivated lands were examined. The main objective was to assess the feasibility of using the PBSA/starch-type composite as a material for a “controlled-release” film bag system to apply bacteria-promoted fertilizer.

## MATERIALS AND METHODS

**Microorganism and Culture Medium.** *B. cepacia* (BCRC 14256) was supplied by the Bioresource Collection and Research Center in Taiwan and cultivated at 37 °C and 200 rpm in nutrient broth (NB) (Merck KGaA, Darmstadt, Germany). The broth consisted of 3 g of beef extract, 5 g of peptone, and 1.0 L of distilled water at a pH of 7.0. The culture was collected in its early stationary phase for cell entrapment.

**Materials.** The PBSA was supplied by Mitsubishi Chemical Co. Ltd. (Tokyo, Japan) and had an average molecular weight ( $M_w$ ) of  $1.53 \times 10^5$ , a polydispersity index of 1.86, and an intrinsic viscosity ( $\eta$ ) of 2.63 dL/g. MA, obtained from Sigma (St. Louis, MO), was purified before use by recrystallization from chloroform. Benzoyl peroxide (BPO; Sigma) was used as an initiator and was purified by dissolution in chloroform and reprecipitation in methanol. The starch (Sigma) used in the composites was a corn starch composed of 27% amylose and 73% amylopectin, with a granule size of 15–100  $\mu\text{m}$ . PBSA-g-MA was synthesized according to previously published procedures (11) and had a  $M_w$  of  $1.21 \times 10^5$ , a polydispersity index of 2.23, and a  $\eta$  of 2.48 dL/g. The grafting percentage of PBSA-g-MA was approximately 1.08 wt %. At such a low degree of grafting, the PBSA-g-MA structure was not noticeably different from that of PBSA. A slight decrease in  $M_w$  and intrinsic viscosity was apparent in PBSA-g-MA compared to PBSA and was attributable to bond cracking induced by the grafting reaction.

**Sample Preparation.** MA was grafted onto PBSA dissolved in a tetrahydrofuran solution under a nitrogen atmosphere at  $50 \pm 2$  °C, and the polymerization reaction was initiated with 0.3 wt % BPO. The reaction system was stirred at 60 rpm for 8 h. The grafted product (4 g) was then dissolved in 200 mL of refluxing tetrahydrofuran at  $50 \pm 2$  °C, and the hot solution was filtered through several layers of cheesecloth. The cheesecloth was washed with 600 mL of acetone to remove the tetrahydrofuran-insoluble unreacted MA, and the product remaining on the cheesecloth was dried in a vacuum oven at 80 °C for 24 h. The tetrahydrofuran-soluble product in the filtrate was extracted 5 times using 600 mL of cold acetone for each extraction. Subsequently, the grafting percentage was determined using a titration method (19). The titration revealed a grafting percentage of about 1.08 wt %. BPO and MA loadings were maintained at 0.3 and 10 wt %, respectively.

The starch was dried in an oven at 105 °C for 24 h and blended at a fixed 20 wt % with PBSA-g-MA via the melt blending method using a Plastograph 200 N m mixer (W50EHT; Brabender GmbH, Duisburg, Germany) with a blade-type rotor. A predetermined amount of PBSA-g-MA was placed into the Brabender instrument for melting at 50 rpm and

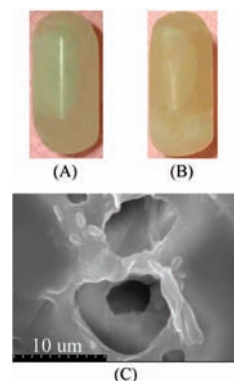


**Figure 1.** (A and B) Photographs of the PBSA and PBSA-g-MA/starch matrix, respectively, loaded with a fixed volume (1.5 mL) of *B. cepacia* and (C) SEM micrograph of PBSA-g-MA/starch (20 wt %) matrix loaded with *B. cepacia* for 10 days.

100 °C. When the PBSA-g-MA had melted completely, a preweighed amount of the dried starch was added into the mixer and blended for 15 min. The product was formed into 1 mm plates using a hot press, which were placed in a dryer for cooling. The thin plates were then made into standard specimens for characterization.

**Cell Release Experiments, the Measurement of the Cell Concentration, and Fertilizer Test.** The cell-loaded film bags were suspended in saline solution (0.85% NaCl), and the cell concentration in the solution was monitored over time. The cell concentration was determined by counting the colony-forming units (CFUs) present on NB agar plates after serial dilution and an overnight incubation at 30 °C.

For the controlled-release bacterial test, film bags (1.00 cm diameter  $\times$  2.50 cm length  $\times$   $0.15 \pm 0.03$  mm thickness) were prepared from conditioned PBSA or a PBSA-g-MA/starch matrix by the film bag model and a fixed volume (1.5 mL) of *B. cepacia* containing 2.8 mg of cells (ca.  $2.3 \times 10^9$  cells) was injected into the film bags by syringes (panels A and B of Figure 1). The cell-loaded film bags were immersed into sterile saline solution (0.85% NaCl) with an initial pH of 7.0 and incubated at 37 °C. Under such conditions, Figure 1C shows that *B. cepacia* was a rod-shaped bacterium of  $0.9\text{--}2.5 \times 0.5\text{--}1.0$   $\mu\text{m}$  and noticeable degradation was seen for the PBSA-g-MA/starch (20 wt %) matrix that encapsulated *B. cepacia* cells for 30 days, suggesting that the bacteria entrapped in the composites were still alive and possessed normal functioning under a phosphate-solubilizing condition. The extent of film bag degradation was monitored at designated 10 day time intervals. The cell concentration in the solution was determined by counting the CFUs present on NB agar plates after a serial dilution and an overnight incubation at 30 °C, thereby allowing the release of cells to be assessed.

On the other hand, to compare the effect of *B. cepacia* in fertilizer, BEFB (Figure 1B) was suspended in 150 mL of fertilizer solution. The fertilizer was inorganic compound fertilizer (N/P/K = 1:3:2) (Taiwan Horticultural Co. Ltd., Taipei, Taiwan), and 1 g of fertilizer was dissolved in 1 L of water. Figure 2A shows the surface morphology of fertilizer particles (6–11  $\mu\text{m}$ ) without BEFB and the size of the fertilizer particles almost without any variation after 40 days (Figure 2C). However, the fertilizer particle paste spread after 40 days with the addition of BEFB. According to the results, *B. cepacia* can degrade the particle of fertilizer into slight ones and make fertilizer easier to be absorbed by plants. The results can also be proven by the plant growth test shown in the following sections.

**Plant Growth Test.** Lily (*Sorbonne lilium*, Holland) was studied by evaluating the growth of the flower over time in a soil environment. The growing medium consisted of soil and fertilizer in a flowerpot. Fertilizer was adjusted to pH  $6.1 \pm 0.5$ , with the temperature maintained between  $21 \pm 5$  °C (day) and  $16 \pm 4$  °C (night), and all plants received full natural sunlight. Soil was cultivating soil (consisting of peat moss, humus, snake-wood, and perlite) (Shen Hong Co. Ltd., Taipei, Taiwan) and was sifted to remove large clumps and plant debris. Procedures used for soil burial were the same as those described by Piotr et al. (20). Soil was maintained at approximately 40% moisture in weight, and film bag samples (Figure 1B) were buried at a depth of  $4 \pm 2$  cm. A control flowerpot consisted of only

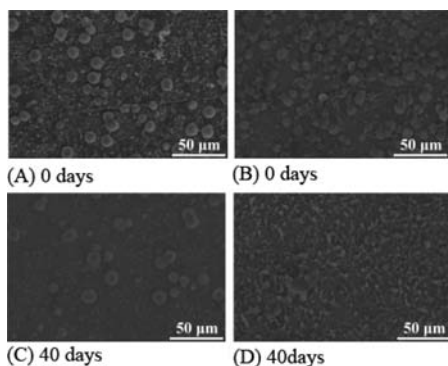


**Figure 2.** SEM surface morphology of fertilizer particles without BEFB for (A) 0 day and (C) 40 days and fertilizer particles with BEFB for (B) 0 day and (D) 40 days (600 $\times$ ).

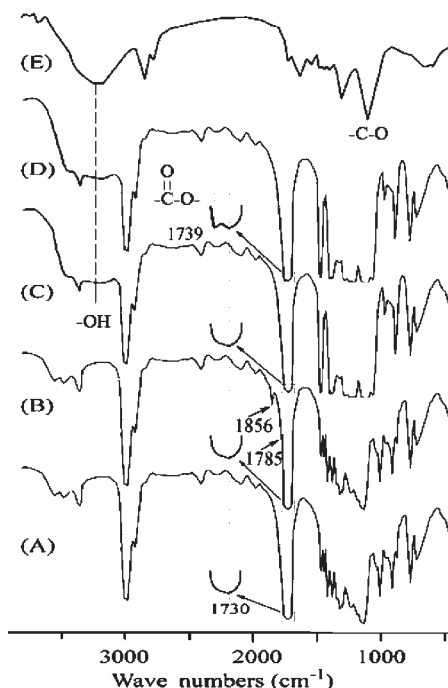


**Figure 3.** FTIR spectroscopy spectra of (A) PBSA, (B) PBSA-*g*-MA, (C) PBSA/starch (20 wt %), (D) PBSA-*g*-MA/starch (20 wt %), and (E) starch.

the plant and soil, in contrast with the growing conditions of the plant with added BEFB.

**Characterization of PBSA and PBSA-*g*-MA/Starch.** Solid-state  $^{13}\text{C}$  nuclear magnetic resonance (NMR) was performed with an AMX-400 NMR spectrometer (Bruker, Billerica, MA) at 100 MHz under cross-polarization while spinning at the magic angle (21). Power decoupling conditions were set with a 90° pulse and a 4 s cycle time. FTIR sample spectra were obtained using a FTS-7PC-type Fourier transform infrared (FTIR) spectrophotometer (Bio-Rad, Hercules, CA), whereas gel-permeation chromatography (GPC) was performed at 40 °C using a Perkin-Elmer series 200 system (Waltham, MA) equipped with a gel divinylbenzene 10000As instrument (Jordi, Bellingham, MA), gel columns with a refractive index detector RI-71 (Shodex, Tokyo, Japan) as the detector, and polystyrene as the standard.

A capillary viscometer (Schott AG, Mainz, Germany) was used to measure the intrinsic viscosity of PBSA or PBSA-*g*-MA/starch dissolved in a chloroform solvent at various concentrations (0.5, 1.0, 1.5, and 0.2 g/dL). The solutions were cleared through a 0.45  $\mu\text{m}$  filter (Lida, Kenosha, WI), and then the capillary viscometer was filled with 10 mL of sample and equilibrated in a water bath (B801; Schott AG) at  $30 \pm 0.5$  °C. Each sample was passed through the capillary tube once before flow time was measured. The flow time was used to calculate the relative and reduced

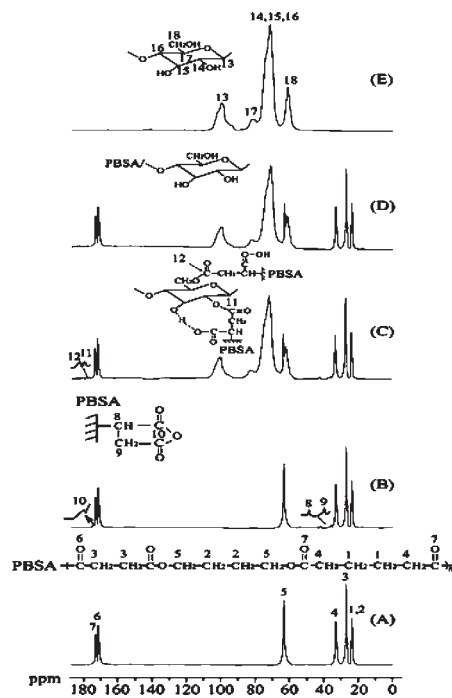


**Figure 4.**  $^{13}\text{C}$  NMR spectra of (A) PBSA, (B) PBSA-*g*-MA, (C) PBSA/starch (20 wt %), (D) PBSA-*g*-MA/starch (20 wt %), and (E) starch.

viscosities, which were plotted against the concentration, and the intercept was the intrinsic viscosity. After the samples were treated with glutaraldehyde and then immersed in 50–100% acetone solutions, the samples were dried at 50 °C for 48 h and coated with gold and then their morphology was observed with a scanning electron microscope (SEM; model S-4100; Hitachi, Tokyo, Japan) (22).

## RESULTS AND DISCUSSION

**Characterization of PBSA and PBSA-*g*-MA/Starch Film Bag Material.** To identify the structure difference between PBSA and modified PBSA/starch, FTIR and NMR were used to characterize the film bag material. The FTIR spectra of unmodified PBSA and PBSA-*g*-MA are shown in curves A and B of Figure 3, respectively. The characteristic transitions of PBSA at 3300–3700, 1700–1760, and 500–1500  $\text{cm}^{-1}$  appeared in the spectra of both polymers, with two extra shoulders observed at 1785 and 1856  $\text{cm}^{-1}$  in the modified PBSA spectrum. These features are characteristic of anhydride carboxyl groups. Similar results have been reported previously (23, 24). The shoulders represent free acid in the modified polymer and, therefore, denote the grafting of MA onto PBSA. The starch FTIR spectrum (Figure 3E) exhibited peaks at 3241 and 1063  $\text{cm}^{-1}$  attributable to hydroxyl groups and –CO stretching, respectively (25).

The peak assigned to the –OH stretching vibration at 3200–3700  $\text{cm}^{-1}$  intensified in the composite PBSA/starch (20 wt %) (Figure 3C) because of contributions from the –OH group of starch. The FTIR spectrum of the PBSA-*g*-MA/starch (20 wt %) composite revealed a peak at 1737  $\text{cm}^{-1}$  that was not present in the FTIR spectrum of the PBSA/starch (20 wt %) composite (Figure 3D). This peak was assigned to the ester carbonyl stretching vibration of the co-polymer. Yoshimura et al. (26) also reported an absorption peak at 1735  $\text{cm}^{-1}$  for this ester carbonyl group. These data suggest the formation of branched and cross-linked macromolecules in the PBSA-*g*-MA/starch by a covalent reaction of the anhydride carboxyl groups in PBSA-*g*-MA with the hydroxyl groups of starch.

To further confirm this finding, solid-state  $^{13}\text{C}$  NMR spectra of PBSA and PBSA-*g*-MA were compared in panels A and B of Figure 4, respectively. Three peaks were observed corresponding



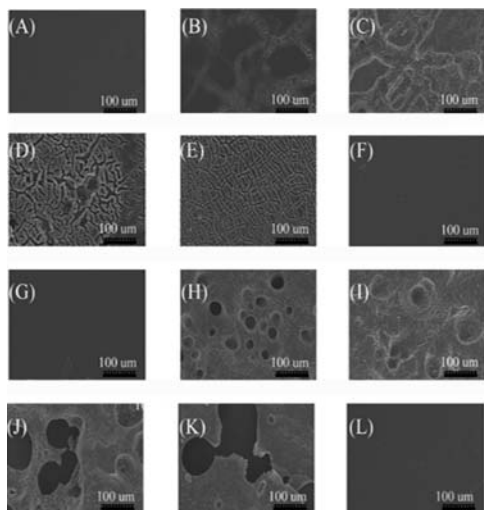


**Figure 5.** Time-course SEM morphology of the PBSA matrix loaded with *B. cepacia* cells (magnification of 300 $\times$ ): (A) 0 days, (B) 10 days, (C) 20 days, (D) 40 days, (E) 60 days, and (F) cell-free PBSA matrix (60 days). Time-course morphology of the PBSA-g-MA/starch (20 wt %) matrix loaded with *B. cepacia* cells (magnification of 300 $\times$ ): (G) 0 days, (H) 10 days, (I) 20 days, (J) 40 days, (K) 60 days, and (L) cell-free PBSA-g-MA matrix (60 days).

to carbon atoms in the unmodified PBSA (1 and 2,  $\delta = 24.6$  ppm; 3,  $\delta = 28.7$  ppm; 4,  $\delta = 33.6$  ppm; 5,  $\delta = 63.2$  ppm; 6,  $\delta = 171.3$  ppm; and 7,  $\delta = 172.7$  ppm) (18). The  $^{13}\text{C}$  NMR spectrum of PBSA-g-MA showed additional peaks (8,  $\delta = 42.3$  ppm; 9,  $\delta = 36.2$  ppm; and 10,  $-\text{C}=\text{O}$ ,  $\delta = 173.5$  ppm), thus confirming that MA was grafted covalently onto PBSA.

The solid-state  $^{13}\text{C}$  NMR spectra of PBSA/starch (20 wt %), PBSA-g-MA/starch (20 wt %), and starch are shown in panels C–E of Figure 4, respectively. Relative to unmodified PBSA, additional peaks were observed in the spectra of composites containing PBSA-g-MA. These additional peaks were located at  $\delta = 42.3$  and 36.2 ppm. These same features were observed in previous studies (27) and indicate grafting of MA onto PBSA. However, the peak at  $\delta = 173.5$  ppm ( $\text{C}=\text{O}$ ) (Figure 4B), which is also typical for MA grafted onto PBSA, was absent in the solid-state PBSA-g-MA/starch spectrum (20 wt %). This occurrence was most likely the result of an additional condensation reaction between the anhydride carboxyl group of MA and the  $-\text{OH}$  group of starch that caused the peak at  $\delta = 173.5$  ppm to split into two bands ( $\delta = 176.8$  and 178.1 ppm). This additional reaction converted the fully acylated groups in the original starch to esters (represented by peaks 11 and 12 in Figure 4C) and did not occur between PBSA and starch, as indicated by the absence of corresponding peaks in the FTIR spectrum of PBSA/starch (20 wt %) (Figure 4D). The formation of ester groups significantly affects the thermal and biodegradation properties of PBSA-g-MA/starch and is discussed in greater detail in the following sections.

**Biodegradation of PBSA and PBSA-g-MA/Starch Composite by *B. cepacia*.** *B. cepacia* is a rod-shaped bacterium with a size of  $0.9\text{--}2.5 \times 0.5\text{--}1.0 \mu\text{m}$ . The time-course changes in the morphology of the PBSA and PBSA-g-MA/starch matrices that encapsulated *B. cepacia* cells focused on 10, 40, and 60 days (Figure 5).

At 10 days, cell growth occurred on the surface of the PBSA matrix (Figure 5B). Moreover, some erosion and cracking were observed on the matrix surface. At 40 days, the disruption of the PBSA matrix structure was more apparent (Figure 5D). This degradation was confirmed by an increasing weight loss of the PBSA matrix with incubation time (Figure 6A) and reached

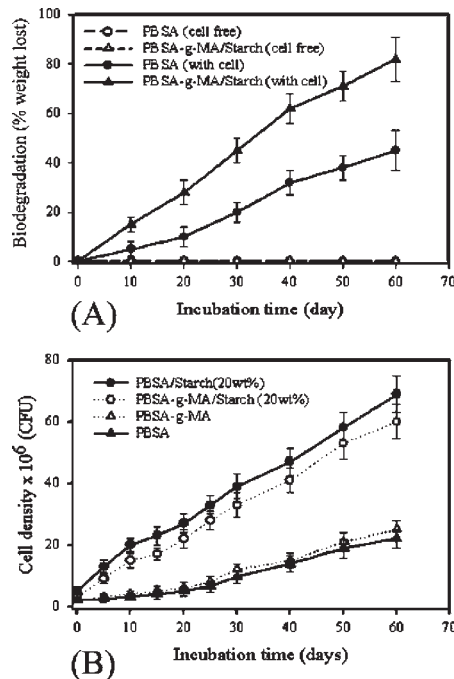


**Figure 6.** (A) Time course for biodegradation (percent weight loss) of PBSA and PBSA-g-MA/starch (20 wt %) loaded with *B. cepacia* cells. (B) Time-course release and growth of *B. cepacia* cells entrapped in PBSA, PBSA-g-MA, PBSA/starch (20 wt %), and the PBSA-g-MA/starch (20 wt %) matrix suspended in saline solution.

nearly 45% after 60 days. The most likely cause of this weight loss was biodegradation by *B. cepacia*, because the PBSA is biodegradable. Reports in the literature have described bacterial degradation of PBSA (28, 29), and some of the degradation was attributable to a variety of enzymes, such as lysozyme (14, 30). These results show that *B. cepacia* is somewhat effective for degrading PBSA.

The PBSA-g-MA/starch (20 wt % of starch) composite appeared to be degraded more easily by *B. cepacia*. At 10 days, a biofilm of bacterial cells was seen on the surface of the PBSA-g-MA/starch (Figure 5H), implying more abundant cell growth than on PBSA at 10 days. Moreover, larger pores were observed on the PBSA-g-MA/starch composite at 40 and 60 days (panels J and K of Figure 5), indicating a higher level of destruction. The weight loss of the PBSA-g-MA/starch composite was also accelerated compared to that of PBSA and exceeded 82% after 60 days (Figure 6A).

These results clearly indicate that the addition of starch enhances the biodegradability of the composite and may thereby facilitate the release of the entrapped cells into the environment. Hence, the release of BEFB can be controlled by the addition of biodegradable supplements (e.g., starch) into the core matrix, with higher levels of supplement leading to a more rapid release.

**Cell Release from PBSA and PBSA-g-MA/Starch Composite Encapsulating *B. cepacia*.** The foregoing results indicated significant bacterial destruction of the matrix during the course of the incubation. Therefore, the time-course profile for cell release was examined. After a 60 day incubation, the final cell concentration in the saline solution was between  $2.2 \times 10^7$  and  $6.9 \times 10^7$  CFU/mL (Figure 6B), indicating that cells were released into the solution and remained viable. The cell-release pattern was similar for PBSA and the PBSA-g-MA/starch matrix, whereas the amount and rate of release were different. Figure 6B shows that the rate of cell release as represented by CFUs was noticeably

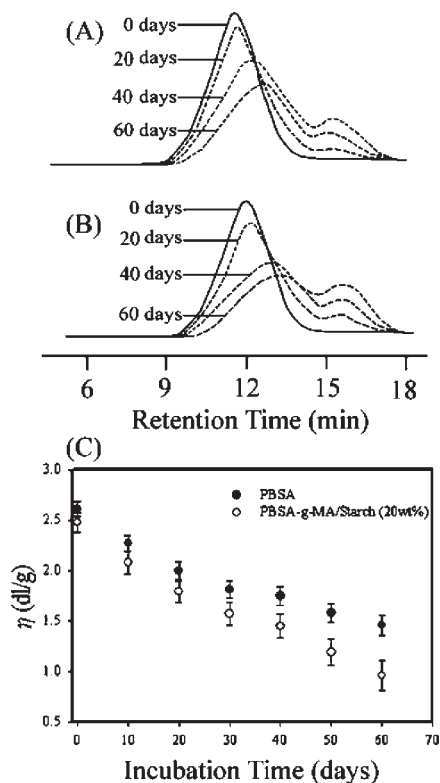


**Figure 7.** (A and B) Time-course profile of the retention time in the GPC analysis for PBSA and PBSA-g-MA/starch loaded with *B. cepacia* cells. (C) Time-course profile of the intrinsic viscosity for PBSA and PBSA-g-MA/starch loaded with *B. cepacia* cells.

lower in the first 20 days than in the remaining incubation period, especially for the PBSA/starch and PBSA-g-MA/starch composites. During this earlier period, the increase in the cell concentration was likely due to the release of cells from leaks in the matrix. Then, after being released, the cells in the saline solution may have become inactive or lysed because of the lack of substrate, resulting in a decrease in viable cell concentration and CFUs. The noticeable increase in CFUs from 20 days onward may represent not only an increase in cell release but also an increase in substrate. According to the SEM micrographs (Figure 5), the matrix structure was damaged severely after 20 days, leading to the release of cells as well as residual starch and PBSA fragments or the PBSA-g-MA matrix into the solution; these fragments may then have acted as a substrate to facilitate cell growth. Starch is more readily biodegradable than PBSA, and the solution containing PBSA/starch and the PBSA-g-MA/starch matrix reached a higher final cell concentration with a more rapid increase in the cell concentration between 20 and 60 days. The addition of starch clearly had a positive effect on the number of cells released. As a result, the rate and number of cells released can be adjusted by altering the composition of the matrix materials.

**Time-Course Measurement of GPC and Intrinsic Viscosity.** The biodegraded PBSA and PBSA-g-MA/starch composite samples were also analyzed using GPC, and the results are presented in panels A and B of Figure 7. The retention time of the major peaks (representing the original samples) increased with an increasing incubation time because molecules within the original samples were continuously severed during the biodegradation process. Hence, the longer retention time of PBSA-g-MA/starch also demonstrates that it is more biodegradable than PBSA. Additionally, a new peak appeared at about 15.5 min after 20 days of incubation, suggesting that some fragments were generated

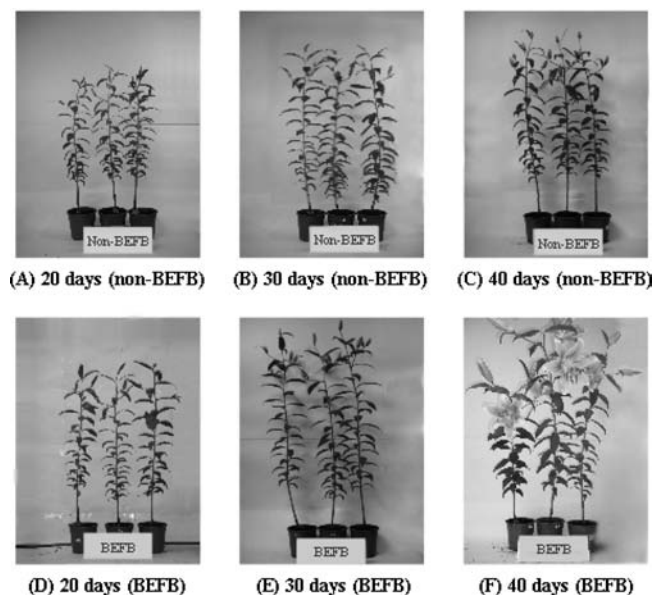


**Figure 8.** Time-course changes in the morphology of the plant growing for (A) 20 days, (B) 30 days, (C) 40 days without BEFB and for (D) 20 days, (E) 30 days, (F) 40 days with BEFB (2.0 $\times$ ).

during the biodegradation of PBSA and PBSA-g-MA/starch composites. The formation of fragments also implies that starch had been nearly depleted by this time. Ratto et al. (31) reported similar results. The retention time of the fragments was approximately invariant, which may have been due to the use of the depolymerized matrix as a substrate by the bacterium, which produced nearly uniform fragments.

The change in intrinsic viscosity and molecular weight with incubation time for PBSA and the PBSA-g-MA/starch composite is given in Figure 7C. The results show that the intrinsic viscosity for PBSA encapsulating *B. cepacia* ranged from 2.61 to 1.46 g/dL over the 0–60 days of incubation, whereas the values for PBSA-g-MA/starch were 2.48–0.97 g/dL. The lower intrinsic viscosity of the latter suggests that more fragments were present. Another cause of the decreased intrinsic viscosity of PBSA-g-MA/starch is the conformational change in the starch molecule caused by the previously discussed formation of an ester functional group. In a study of biodegradation of PBSA by Seretoudi et al. (32), the intrinsic viscosity of esterified PBSA also fell with an increase in the random hydrolysis of the ester group.

**Time-Course Measurement of Plant Growth.** The time-course changes in the morphology of the plant growing with BEFB (PBSA-g-MA/starch matrices) were focused on 20, 30, and 40 days (Figure 8). When the growth rate of plants was compared between 20 and 40 days, the plants with BEFB (panels D–F of Figure 8) flourish more than those without BEFB (panels A–C of Figure 8). These results show that, when BEFB was degraded and *B. cepacia* was released, the culture was effective for degrading fertilizer. The result conforms to Figure 2 that the *B. cepacia* culture can spread the particle of fertilizer into slight ones and make fertilizer easier to absorb by plants. In conclusion, the time-course controlling the addition of BEFB can effectively improve the absorbability of fertilizer, hence promoting the growth, for plants. In addition, it can avoid the phosphate in excess fertilizer that leads to the phenomenon of poor soils.

#### ACKNOWLEDGMENT

The author thanks the Bioresource Collection and Research Center (BCRC) for providing necessary bacterium.

## LITERATURE CITED

- (1) Kidd, P. S.; Domínguez-Rodríguez, M. J.; Díez, J.; Monterroso, C. Bioavailability and plant accumulation of heavy metals and phosphorus in agricultural soils amended by long-term application of sewage sludge. *Chemosphere* **2007**, *66*, 1458–1467.
- (2) Liu, C. H.; Wu, J. Y.; Chang, J. S. Diffusion characteristics and controlled release of bacterial fertilizers from modified calcium alginate capsules. *Bioresour. Technol.* **2008**, *99*, 1904–1910.
- (3) Wu, C. S. Characterizing biodegradation of PLA and PLA-g-AA/starch films using a phosphate-solubilizing *Bacillus* species. *Macromol. Biosci.* **2008**, *8*, 560–567.
- (4) Tao, G. C.; Tian, S. J.; Cai, M. Y.; Xie, G. H. Phosphate-solubilizing and -mineralizing abilities of bacteria isolated from soils. *Pedosphere* **2008**, *18*, 515–523.
- (5) Hilda, R.; Reynaldo, F. Phosphate solubilizing bacteria and their role in plant growth promotion. *Biotechnol. Adv.* **1999**, *17*, 319–339.
- (6) Junli, H.; Xiangui, L.; Junhua, W.; Haiyan, C.; Rui, Y.; Jiabao, Z. Population size and specific potential of P-mineralizing and -solubilizing bacteria under long-term P-deficiency fertilization in a sandy loam soil. *Pedobiologia* **2009**, *53*, 49–58.
- (7) Vassilev, N.; Vassileva, M.; Fenice, M.; Federici, F. Immobilized cell technology applied in solubilization of insoluble inorganic (rock) phosphates and P plant acquisition. *Bioresour. Technol.* **2001**, *79*, 263–271.
- (8) Son, H. J.; Park, G. T.; Cha, M. S.; Heo, M. S. Solubilization of insoluble inorganic phosphates by a novel salt- and pH-tolerant *Pantoea agglomerans* R-42 isolated from soybean rhizosphere. *Bioresour. Technol.* **2006**, *97*, 204–210.
- (9) Kim, H. S.; Kim, H. J.; Lee, J. W.; Choi, I. G. Biodegradability of bio-flour filled biodegradable poly(butylene succinate) bio-composites in natural and compost soil. *Polym. Degrad. Stab.* **2006**, *91*, 1117–1127.
- (10) Zhao, J. H.; Wang, X. Q.; Zeng, J.; Yang, G.; Shi, F. H.; Yan, Q. Biodegradation of poly(butylene succinate-co-butylene adipate) by *Aspergillus versicolor*. *Polym. Degrad. Stab.* **2005**, *90*, 173–179.
- (11) Wu, C. S. Physical properties and biodegradability of maleated-polycaprolactone/starch composite. *Polym. Degrad. Stab.* **2003**, *80*, 127–134.
- (12) Nair, L. S.; Laurencin, C. T. Biodegradable polymers as biomaterials. *Prog. Polym. Sci.* **2007**, *32*, 762–798.
- (13) Ha, C. S.; Cho, W. J. Miscibility, properties, and biodegradability of microbial polyester containing blends. *Prog. Polym. Sci.* **2002**, *27*, 759–809.
- (14) Shah, A. A.; Hasan, F.; Hameed, A.; Ahmed, S. Biological degradation of plastics: A comprehensive review. *Biotechnol. Adv.* **2008**, *26*, 246–265.
- (15) Avérous, L.; Fringant, C. Association between plasticized starch and polyesters: Processing and performances of injected biodegradable systems. *Polym. Eng. Sci.* **2001**, *41*, 727–734.
- (16) Yu, L.; Dean, K.; Yuan, Q.; Chen, L.; Zhang, X. Effect of compatibilizer distribution on the blends of starch/biodegradable polyesters. *J. Appl. Polym. Sci.* **2007**, *103*, 812–818.
- (17) Wu, C. S. Renewable resource-based composites of recycled natural fibers and maleated polylactide Bioplastic: Characterization and biodegradability. *Polym. Degrad. Stab.* **2009**, *94*, 1076–1084.
- (18) Ahn, B. D.; Kim, S. H.; Kim, Y. H.; Yang, J. S. Synthesis and characterization of the biodegradable copolymers from succinic acid and adipic acid with 1,4-butanediol. *J. Appl. Polym. Sci.* **2001**, *82*, 2808–2826.
- (19) Nabar, Y.; Raquez, J. M.; Dubois, P.; Narayan, R. Production of starch foams by twin-screw extrusion: Effect of maleated poly(butylene adipate-co-terephthalate) as a compatibilizer. *Biomacromolecules* **2005**, *6*, 807–817.
- (20) Piotr, R.; Robert, B.; Barbara, H.; Aleksandra, S.; Piotr, K.; Grazyna, A.; Marek, K. Environmental degradation of polyester blends containing atactic poly(3-hydroxybutyrate). Biodegradation in soil and ecotoxicological impact. *Biomacromolecules* **2006**, *7*, 3125–3131.
- (21) Smits, A. L. M.; Kruiskamp, P. H.; van Soest, J. J. G.; Vliegthart, J. F. G. Interaction between dry starch and plasticisers glycerol or ethylene glycol, measured by differential scanning calorimetry and solid state NMR spectroscopy. *Carbohydr. Polym.* **2003**, *53*, 409–416.
- (22) Carmen Gómez-Guillén, M.; Montero, P.; Teresa Solas, M.; Pérez-Mateos, M. Effect of chitosan and microbial transglutaminase on the gel forming ability of horse mackerel (*Trachurus* spp.) muscle under high pressure. *Food Res. Int.* **2005**, *38*, 103–110.
- (23) John, J.; Tang, J.; Yang, Z.; Bhattacharya, M. Synthesis and characterization of anhydride-functional polycaprolactone. *J. Polym. Sci., Part A: Polym. Chem.* **1997**, *35*, 1139–1148.
- (24) Yin, J.; Zhang, J.; Yao, Y. Melt grafting of poly(ethylene-vinyl acetate) copolymer with maleic anhydride. *J. Appl. Polym. Sci.* **2006**, *102*, 841–846.
- (25) Rivero, I. E.; Balsamo, V.; Müller, A. Microwave-assisted modification of starch for compatibilizing LLDPE/starch blends. *Carbohydr. Polym.* **2009**, *75*, 343–350.
- (26) Yoshimura, T.; Yoshimura, R.; Seki, C.; Fujioka, R. Synthesis and characterization of biodegradable hydrogels based on starch and succinic anhydride. *Carbohydr. Polym.* **2006**, *64*, 345–349.
- (27) Gayload, N. G.; Nagler, M.; Watterson, A. C. Structure of alternating *cis*- and *trans*-piperylene-maleic anhydride copolymers by <sup>13</sup>C-NMR analysis. *Eur. Polym. J.* **1983**, *19*, 877–879.
- (28) Pan, P.; Inoue, Y. Polymorphism and isomorphism in biodegradable polyesters. *Prog. Polym. Sci.* **2009**, *34*, 605–640.
- (29) Tezuka, Y.; Ishii, N.; Kasuya, K. I.; Mitomo, H. Degradation of poly(ethylene succinate) by mesophilic bacteria. *Polym. Degrad. Stab.* **2004**, *84*, 115–121.
- (30) Ishii, N.; Inoue, Y.; Tagaya, T.; Mitomo, H.; Nagai, D.; Kasuya, K. I. Isolation and characterization of poly(butylene succinate)-degrading fungi. *Polym. Degrad. Stab.* **2008**, *93*, 883–888.
- (31) Ratto, J. A.; Stenhouse, P. J.; Auerbach, M.; Mitchell, J.; Farrell, R. Processing, performance and biodegradability of a thermoplastic aliphatic polyester/starch system. *Polymer* **1999**, *40*, 6777–6788.
- (32) Seretoudi, G.; Bikiaris, D.; Panayiotou, C. Synthesis, characterization and biodegradability of poly(ethylene succinate)/poly(*ε*-caprolactone) block copolymers. *Polymer* **2002**, *43*, 5405–5415.

---

Received for review October 13, 2009. Accepted March 18, 2010. The author was grateful to the Agriculture and Food Agency, Council of Agriculture, Executive Yuan, Republic of China, for the financial support.